

High Degree of Freedom Hand Pose Tracking Using Limited Strain Sensing and Optical Training

Wentai Zhang[‡] Jonelle Z. Yu[‡]

Zhangsihao Yang[‡] Nurcan Gecer Ulu[‡]

[‡] Carnegie Mellon University, Pittsburgh, PA, USA

Fangcheng Zhu[‡] Yifang Zhu[‡]

Batuhan Arisoy[†]

Levent Burak Kara^{*‡}

[†] Siemens Corporate Technology, Princeton, NJ, USA

The ability to track human operators' hand usage when working in production plants and factories is critically important for developing realistic digital factory simulators as well as manufacturing process control. We propose an instrumented glove with only a few strain gauge sensors and a micro-controller that continuously tracks and records the hand configuration during actual use. At the heart of our approach is a trainable system that can predict the fourteen joint angles in the hand using only a small set of strain sensors. First, ten strain gauges are placed at the various joints in the hand to optimize the sensor layout using the English letters in the American Sign Language as a benchmark for assessment. Next, the best sensor configurations for three through ten strain gauges are computed using a support vector machine classifier. Following the layout optimization, our approach learns a mapping between the sensor readouts to the actual joint angles optically captured using a Leap Motion system. Five regression methods including linear, quadratic and neural regression are then used to train the mapping between the strain gauge data and the corresponding joint angles. The final proposed model involves four strain gauges mapped to the fourteen joint angles using a two-layer feed-forward neural network.

1 Introduction

Recent advances in 3D data acquisition and tracking technologies have enabled a rapid digitalization of large production plants and factories in various formats such as point clouds and triangle soups ([a set of unorganized and disconnected triangles](#)). Acquired data is utilized for the generation of digital twin of manufacturing processes, which can be used to simulate and optimize work-cell layouts while improving human operator effectiveness, safety and ergonomics. Although existing process simulation tools can make use of digitized factory environments in the form of point clouds, these tools still require a labor intensive manual configuring of the simulation environment such as how human workers interact with the assembly tools and how they

manipulate different objects during manufacturing.

In this work, we address the problem of acquiring an accurate 3D model of human hand usage using an instrumented glove with only a few strain gauge sensors. Once available, this data can be incorporated directly into factory environment simulators, thereby alleviating the need for manual process parameter tuning. Specifically, we envision that a set of instrumented gloves will be utilized by human workers while they are performing their jobs in a real factory environment and the proposed wearable device will enable automatic data collection for understanding how human workers interact with their surroundings.

Towards this goal, we develop a wearable device that is able to track and record human hand poses relative to the wrist over an extended period of time. The main advance in this work is the development of methods, algorithms, and a prototype device that use as little as *four* strain gauges to predict in real-time all the *fourteen* joint angles in the fingers with an average RMSE ([root-mean-square error](#)) of 3.6° . Given a target number of strain gauges, we begin by identifying the best layout configuration of these sensors on the outer surface of the human hand using the classification performance on the English letters in American Sign Language as a way to assess candidate layouts. Next, we establish a training protocol for hand pose tracking wherein a new user wears and trains the glove for a duration of 3 minutes. The purpose of this training is to learn a mapping from the sensor readouts to the fourteen joint angles, where the joint angles are captured using a Leap Motion depth sensor as the ground truth. This approach enables high-fidelity benchmark poses to be gathered during the training phase using optical tracking, while alleviating the need for optical tracking during actual use (hence only requiring strain sensing). The results of our experiments involving a varying number of strain gauges as well as regression algorithms involving linear least squares, quadratic least squares and neural regression are also compared. Our studies suggest that an instrumented glove with four strain gauges that uses neural regression to be the best compromise between tracking accuracy and device simplicity.

*Address all correspondences to lkara@cmu.edu

Our main contributions are:

1. A method to identify the best strain sensor layout for human hand pose estimation.
2. A training algorithm between optically captured hand poses and a lower dimensional strain data for high fidelity hand pose tracking.
3. A wearable glove with a limited number of strain sensors for real-time hand pose tracking.

2 Related Work

Our work builds on hand gesture recognition and tracking systems with a specific focus on factory environment use. In this section, we review hardware systems and computational algorithms of two main hand tracking approaches, (1) wearable sensor systems, (2) vision based techniques. Additionally, we discuss commercially available hand tracking systems in relation to our specific problem.

Wearable devices typically integrate strain, acceleration, and force sensors combined with classifiers for hand pose recognition [1–3]. Compared to these works, our aim is to track the full hand pose rather than a set of discrete hand gestures. Kramer [1] present a hand gesture recognition system using an instrumented glove with approximately 20 sensors where each sensor is comprised of two strain gauges. In our approach, we aim to minimize the number of strain sensors for ease of usability and fabrication. The musculoskeletal system of the hand allows the prediction of hand movement (all 14 joints) using fewer number of sensors due to a coupling between the joint angles. In our approach, we exploit this coupling to achieve accurate tracking using only a few sensors (3-5) with a performance similar to 10 strain gauges. Note that this approach requires a special attention due to the mapping from low dimensional sensor data to a high dimensional joint angle space (Section 3.3.2).

Lei et al. [3] presents an accelerometer-based method to detect 12 predefined index finger movements of stroke patients during rehabilitation therapies. The study reports gesture recognition accuracy varying from 59% to 87% and continuous tracking of one finger on the 12 classes. One drawback of accelerometer-based approaches is that these sensors are rigid pieces. In contrast, strain gauges are inherently slimmer, lighter and flexible allowing them to better conform to natural hand poses. Federico [2] demonstrate a glove design with conductive mixture patterns as sensors. While the above study presents very high accuracy at first wear, sensor-based approaches are sensitive to hand sizes and repetitive wears. In our approach, we overcome this issue with a short training session using a depth sensor in a controlled environment.

Vision-based approaches have been widely used in gesture recognition and motion tracking applications. These vision-based approaches have been demonstrated using many different hardware setups including optical or infrared cameras [4, 5], RGB cameras and depth sensors [6, 7]. Gioliu [8] present an SVM based gesture recognition algorithm using infrared cameras, RGB cameras and depth sensors, re-

porting up to 92% accuracy. Real-time hand tracking has been studied in [22]. However, vision based techniques are non-wearable and non-portable settings which are not feasible in an industrial environment. Vision based techniques are also sensitive to environment conditions such as lighting which may change during an operation in a factory. Moreover, vision based techniques are not suitable for hand tracking while holding other objects due to occlusions.

Posture recognition systems for other body parts such as the arm [16], leg [17], and body [18, 19] have also been extensively studied. In principle, these works share techniques and goals similar to that of hand tracking. Yet, the hand tracking problems require higher resolution sensor readings as well as smaller hardware restrictions for portability.

There exists a growing body of commercial hand gesture recognition and tracking systems. Proglove [9] is a wearable device that demonstrates the need for tracking operations in a factory environment. Proglove is designed to scan and display the items which are being touched or handled for industrial logistics, hence is not concerned with hand pose estimation and tracking. Gest (accelerometer-based) and Myo (acoustic-based) [13, 14] are wearable devices that focus on hand gesture recognition to control computers and machines. Compared to these devices, our aim is to develop a wearable system that can be incorporated into traditional work gloves with whole hand tracking capabilities. Cyber Glove [10] is a motion capture device equipped with 22 sensors for full hand tracking. In contrast, understanding redundancies and minimizing the number of sensors is key in our approach to enable development of a comfortable and affordable glove system. In addition, we introduce a training approach for personalized calibration of glove systems.

Leap Motion and Kinect [13, 14] are vision-based hand tracking devices primarily for virtual reality gaming. They require external devices like cameras to be placed facing the tracked objects. Such non-portable settings requiring optical sensors are not feasible in our target context. However, these approaches are very useful for training and calibration purposes. As such, we use a Leap Motion system for the initial mapping of strain sensor data to the joint angles. By combining the strain sensor based tracking with the vision-based pretraining, we can monitor hand poses even when the hand is occluded holding an object and we can quickly train the algorithms for accurate personalized tracking. To our knowledge, our study is the first to focus on real-time hand pose tracking with or without objects in hand using only a few strain sensors.

3 Technical Approach

In this paper, our objective is hand pose tracking using a simple and portable hardware setup and develop algorithms that address our specific challenges. We divide our technical discussions into two parts. First, we discuss the hardware design and explain our algorithms for choosing informative sensor placements. Second, we describe the hand tracking protocol and the training procedure for personalized tracking that captures the hand size and a possible initial deformation

of the strain sensors.

3.1 Hardware Design and Initial Sensor Layout

As shown in Figure 1a, there are 14 joints in the hand. Our approach aims to track the angular deformations at these joints during the hand's actual use. For our prototype, we choose a latex glove in order to achieve a tight fit with the hand as a way to increase strain readout fidelity. For the initial strain gauge placement, we use 10 strain gauges as shown in Figure 1b. We observe that the motion of the tip joints (J5, J8, J11, J14) are strongly coupled with the mid joints (J4, J7, J10, J13) at each finger making two of these joints on the same finger difficult to move independently. Based on this observation, we place only two sensors per finger, resulting on 10 total sensors (S1-S10).

3.1.1 Hardware Setup

For the prototype, 10 strain gauges (KFH-20-120-C1-11L1M2R, Omega) are attached to a medium-sized Latex glove (Microflex Diamond GripTM, ULINE) using double-sided tape. The glove is worn by a human subject and the hand is laid flat on a flat surface prior to attaching the sensors as shown in Figure 1b. This configuration simply establishes a strain-free datum for the sensor network. Any subsequent hand motion is registered via the tensile or compressive strain readouts. Once the sensors are attached, this particular glove is used by all human subjects without changing the sensor locations, with user-specific [training prior to the use of the glove](#) as will be discussed in Section 3.3.

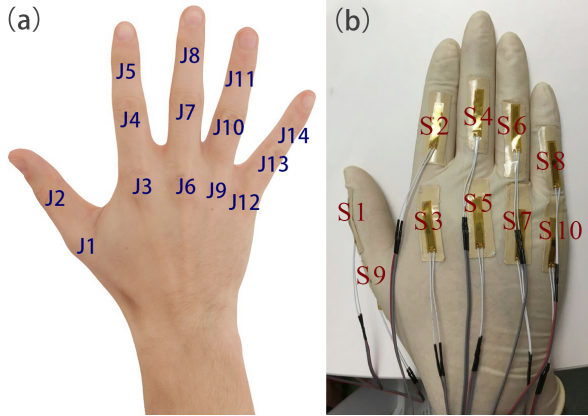


Fig. 1. (a) Fourteen joints in the hand. (b) Ten strain sensor layout on a latex glove.

As shown in Figure 2, we use an Arduino microcontroller board for the strain readouts with a Wheatstone bridge amplifier (INA125P-ND, Texas Instruments), whose output is then channeled to the analog port of the Arduino Mega Board to register the 10 strain gauges.

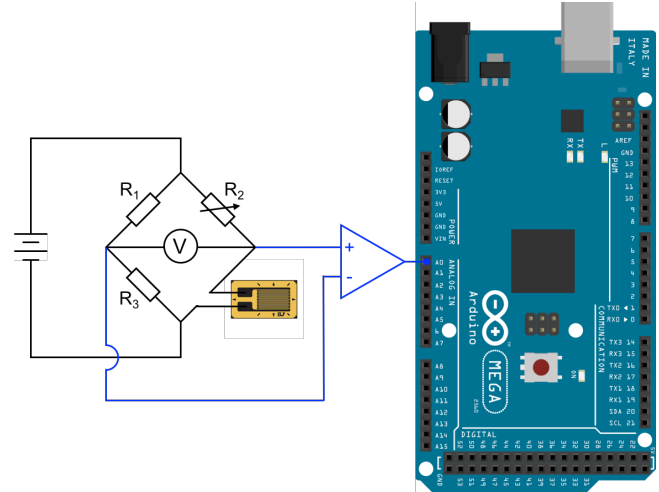


Fig. 2. The schematic design of hardware setup (1 channel).

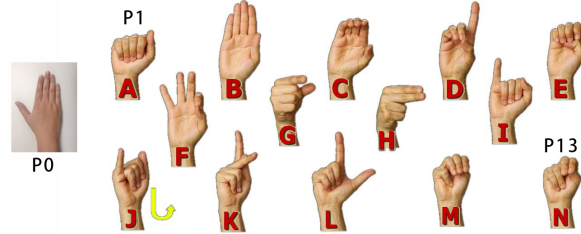


Fig. 3. The hand gestures used in our sensor selection study. P0 corresponds to neutral hand pose that serves as a calibration point. P1 to P13 are the first 13 letters (A-M) in American Sign Language. Image courtesy Dr. Bill Vicars at Lifeprint.com.

3.2 Data Collection and Sensor Layout Optimization

In this section, we explain the data collection and sensor layout selection process to determine which sensor configurations provide the highest information gain as measured through a gesture classification system. This process is repeated for a range of target sensor numbers (3 through 10 sensors). For each target number of sensors, we identify the best strain gauge choices using the classification performance on the English letters in American Sign Language (ASL) as a way to assess the candidate sensor choices (Figure 3). Toward this goal, three users (two males, one female) perform the static gestures for the first 13 letters of the ASL while wearing the instrumented glove. For each user, pose 0 serves as the neutral calibration point to zero all sensor readouts prior to each trial. In each iteration, the user presents pose 1 through pose 13 while holding each pose for approximately 10 seconds. The sensor readouts are recorded at every 100 milliseconds. Each user repeats the experiment for the second time by taking off the glove and wearing it again. Following data collection, the transition periods between the thirteen poses (the leading and trailing two seconds for each pose) are removed.

Next, the data obtained from the three users is aggregated into a large set, separated into two bins: First time wear (all users aggregated) and second time wear (again, all

Table 1. Recognition accuracy of the best five sensor configurations using three strain gauges.

| Configuration | Training Accuracy(%) | Test Accuracy(%) |
|---------------|----------------------|------------------|
| S5,S8,S9 | 98.29 | 63.44 |
| S5,S6,S8 | 95.96 | 59.56 |
| S5,S6,S9 | 93.11 | 58.72 |
| S6,S8,S9 | 90.90 | 57.04 |
| S7,S8,S9 | 94.02 | 50.80 |

users aggregated). The first time wear data is used for training, and is further broken into 10-fold training and validation sets. For each target number of sensors, we use a multi-class support vector machine (SVM) with cross validation to determine the strain gauge combinations that yield the highest user-independent recognition accuracy on the ASL test.

Table 1 shows the recognition accuracy on the ASL data for sensor configurations consisting of only three sensors (top 5 of $C(10)_3$ choices). The training accuracy (trained on first time wear data) reports the average of the validation runs for each configuration, while the test accuracy reports the results on the test set (second time wear data). The fall-off between the training accuracy and test accuracy mainly results from the misalignment among different wearings. As shown, S5, S8 and S9 form the best 3-sensor configuration.

Table 2 summarizes the best sensor choices as a function of the target number of strain gauges.

Table 2. Best sensor configuration for each target number of strain gauges (3 to 9).

| No. of target SGs | Best Configuration |
|-------------------|-----------------------------|
| 3 | S5,S8,S9 |
| 4 | S6,S7,S8,S9 |
| 5 | S5,S6,S7,S8,S9 |
| 6 | S2,S4,S5,S7,S8,S9 |
| 7 | S1,S2,S4,S5,S7,S8,S9 |
| 8 | S1,S2,S3,S5,S6,S7,S8,S9 |
| 9 | S1,S2,S4,S5,S6,S7,S8,S9,S10 |

3.3 Hand Tracking

After we establish the optimal sensor choices, next we describe the hand tracking process. For hand tracking, the key need is to map the strain sensor readouts to the fourteen joint angles through a training protocol, and use this map as a way to predict the hand pose during actual use. However, the main challenge is in the prediction of the high degrees of freedom joint angles from a fewer number of sensor readouts.

3.3.1 Training for Pose Tracking: Data Collection

For training, we establish a map between the strain sensor readouts and the joint angles with the help of the Leap Motion depth sensor (Figure 4). This system allows the capture of all fourteen joint angles in a controlled environment, thus establishing the ground truth for the strain to joint angle mapping.

During training, the users move their hands through random poses while wearing the instrumented glove. The hand motion should be slow enough for strain sensor readings to stabilize against the Leap Motion data capture. Note that this stabilization is only needed during training to match strain sensor readings to Leap Motion data. Hence, no speed restriction is present once the system is trained.

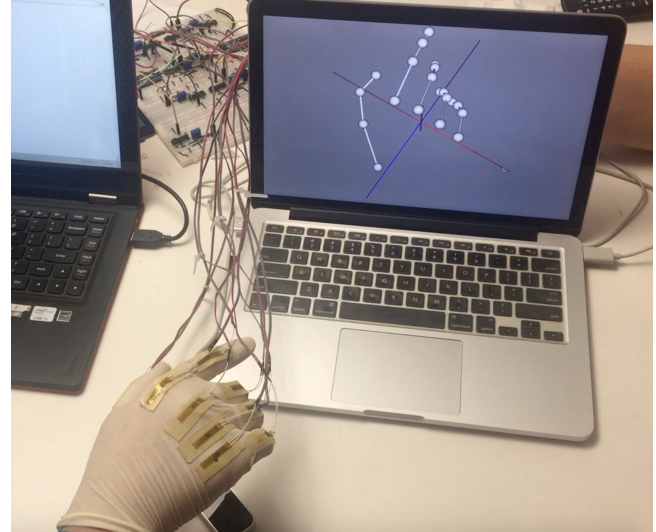


Fig. 4. Optical training process using the Leap Motion system.

Figure 5 shows the amount of variation in each of the fourteen joint angles ($\text{abs}(\text{Angle}_{\max} - \text{Angle}_{\min})$) as captured through the Leap Motion system. These variations are important to note as they will allow an assessment of the RMSE values reported in Section 4.

A new user wears and trains the glove for a duration of 3 minutes. During this phase, the strain readouts and the joint angle readouts are captured at different frequencies, and moreover, the sampling may be non-uniform within each channel. These two input streams are thus registered by acquiring them through the same computer and using the sys-

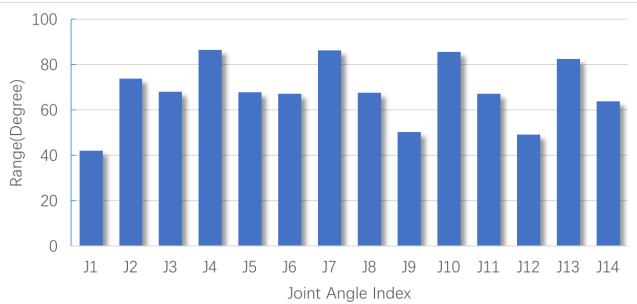


Fig. 5. The range of the joint angles captured through the Leap Motion system.

tem clock as a reference for registration. This produces a large set of registered strain versus joint angle pairs (approximately between 1500 to 1700 pairs) that are used for the next step of training. Note that this training is repeated for each new user to accommodate differences in hand shapes and sizes.

3.3.2 Training Algorithms

To map the strains to the joint angles, we use linear regression, quadratic regression, and feed-forward neural regression. Note that, for these regression models, the mapping is from k strain gauges to the 14 joint angles (where $k < 14$).

Linear Regression: For linear regression with bias, this map can be represented as follows:

$$ST = J \quad (1)$$

where S is the $N \times (k+1)$ strain data matrix (with bias), N is the number of training data points, k is the number of target strain gauges. J is the corresponding $N \times 14$ joint angle matrix encoded in a similar way. T is the desired mapping matrix. We use a linear least squares solver with L_2 regularization to obtain the map T .

Quadratic Regression: Quadratic regression follows a structure similar to that of the linear regression model, except the width of S and the height of T are increased to account for the quadratic terms, while using the same number of training data as before.

Support Vector Regression The Support Vector Regression (SVR) uses the same principles for regression as the Support Vector Machine (SVM) for classification. In our case, we use the Gaussian kernel as the kernel function.

Random Forest Regression Random forest regression is an ensemble learning method for regression that operates by learning a multitude of decision trees whose predictions consolidated into a single prediction [22]. We use 100 decision trees (choice determined empirically) to learn the mapping from the strain sensors to the joint angles.

Neural Regression: Lastly, we build a feed-forward neural network to estimate T . The network admits the strain sensor data as input and estimates the joint angle data on the

output. We train various neural networks with different complexities. Both single and double layer networks are tested, with the number of hidden nodes in each layer ranging from 10, 20, \dots , 50. The sigmoid activation function is used in the hidden layers. Each network is trained three times and is assessed based on the average RMSE.

4 Results and Discussions

In all of our experiments, we trained our algorithms with 90% of shuffled data and tested it with the remaining 10%.

4.1 Neural Network Optimization

We conducted parametric studies to identify the best performing neural network structure. For a single hidden layer, we varied the number of hidden nodes from 5 to 50 with an increment of 5. In all cases, the training continues until an increase in the validation error is observed. The resulting average RMSE values (over different numbers of target input sensors) corresponding to the different number of hidden layer nodes is shown in Figure 6. We deem 15 hidden layer nodes to be a good compromise between network complexity and accuracy.

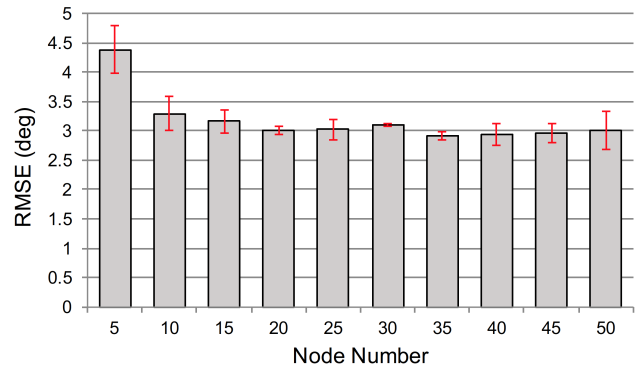


Fig. 6. RMSE for single hidden layer neural networks as a function of hidden nodes.

Similarly, a two hidden layer network was also explored. Here, the number of hidden layer nodes in the first and second hidden layers are varied from 10 to 50 with an increment of 10. Based on the results shown in Figure 7, we choose the network with 10 first layer nodes and 30 second layer nodes (RMSE of 2.73°).

While the optimal single and two hidden layer networks perform well with low RMSE values relative to the joint angle ranges (Figure 6 and 7 versus Figure 5), we use the two hidden layer network over the single hidden layer network in the remainder of this work.

4.2 Comparison of Regression Models

Figure 8 summarizes the performance of our linear (LR), Quadratic (QR), Support Vector (SVR), Random Forest (RFR) and neural network regression (NN) models, reported

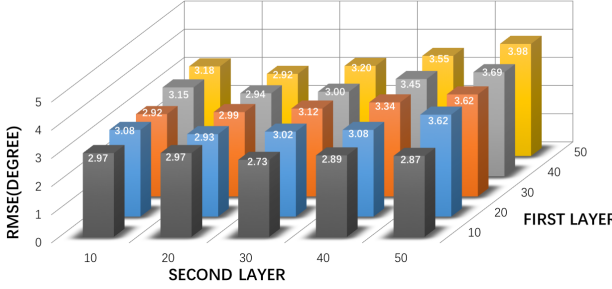


Fig. 7. RMSE for two hidden layer neural networks as a function of hidden layer nodes.

as the RMSE values of the models applied to the test data and averaged over the fourteen joint angles. As shown, QR, **SVR**, **RFR**, and NN produce markedly better estimations over LR (smaller RMSE is better).

For each model, as the number of sensors increases, the RMSE values exhibit a declining trend as expected. Of note is the fact that even with only four sensors, the NN produces results that are better than the ten-sensor models of LR, and QR. The results of NN are slightly better than RFR, and SVR model. With the number of sensors increases, the difference between NN, RFR, and SVR model is becoming smaller. As such, we deem the NN model with four sensors as the best model to deploy with the observed data, as it provides a favorable trade-off between simplicity and test accuracy. As shown in Table 2, this results suggests the use of NN model with strain sensors S6, S7, S8, and S9.

4.3 Insights into the Joints

Figure 9 provides a more detailed view of the RMSE values. In particular, Figure 9 shows - for each joint - the RMSE values for the five regression models for configurations of ten sensors as well as four sensors¹. For most joints, the NN model produces lower RMSE values. Moreover, for the proposed four-sensor configuration (Figure 8 right), the maximum RMSE for the NN is observed at J3 and J6. Interestingly, these two joints also result in the worst RMSE values for LR and QR. And even more interestingly, these joints are also responsible for producing the worst RMSE values for the ten-sensor configuration (Figure 8 left). On the other hand, for RFR and SVR, this observation is reversed. For the four-sensor configuration, for J3, RFR and SVR exhibit better performance over NN. Likewise, when the number of strain gauges is ten, RFR and SVR preform slightly better than NN. This observation offers the insight that combining different regression algorithms using ensembles with respect to different joints may further improve the overall accuracy of our approach.

Figure 10 shows the R^2 values for the five regression models over the different joints. In this case, the higher the R^2 , the better the improvement in the prediction model, compared to the mean model. As seen, the NN model is the best when it comes to explaining the variation in the data.

5 Conclusions

This work presents a trainable instrumented glove that is capable of predicting the fourteen joint angles on a hand using as few as four strain gauges. The long term goal of this study is to enable wearable gloves that can be used in factory settings to monitor workers' hand usage over extended periods of time. The proposed algorithms and prototype system offer a step toward this goal.

During deployment, hand pose prediction that relies solely on strain readouts has the advantage of not being restricted by bulky hardware and other impediments common to optical sensing systems such as object occlusions and lighting. Our work, however, takes a significant advantage of the optical tracking system by offering a short training phase that allows the determination of a robust mapping from the physical strain space to an optically captured joint angle space. The optical tracking is only confined to the training phase, thereby making the proposed system usable during deployment.

Our work has demonstrated that a training duration as short as 3 minutes provides sufficient data to learn a useful mapping from the strain gauges onto the joint angles, thereby making the proposed system practically viable in real-world settings.

While our work uses conventional strain gauges for the development of the methodology, the same infrastructure and algorithmic approach can be immediately adopted for use with more advanced strain sensors with smaller footprints or with those using soft materials and continuous electronic circuitry. We intend to explore this direction as the immediate next step.

5.1 Limitations and Future Work:

Our current study is limited to the prototype glove that includes both sensing and tethered data transmission. An immediate improvement would be to incorporate wireless data transmission. This setup would include a data receiving hardware that connects to the computer system following the same hand tracking algorithms presented in this paper.

Another future direction involves extending glove usage and data collection over durations measured in hours. This way, we can investigate the performance of our hand pose tracking approach for actual use cases with long operational times.

Finally, in future studies, we intend to improve the glove ergonomics, as well as to explore using soft materials and continuous electronic circuitry in the glove to improve comfort. We envision a glove system in which both sensing and circuitry design is further informed by ergonomic considerations.

Acknowledgements

This research is partially funded by Siemens Corporate Technology.

¹Note that Figure 8 reports an average RMSE over these joints.

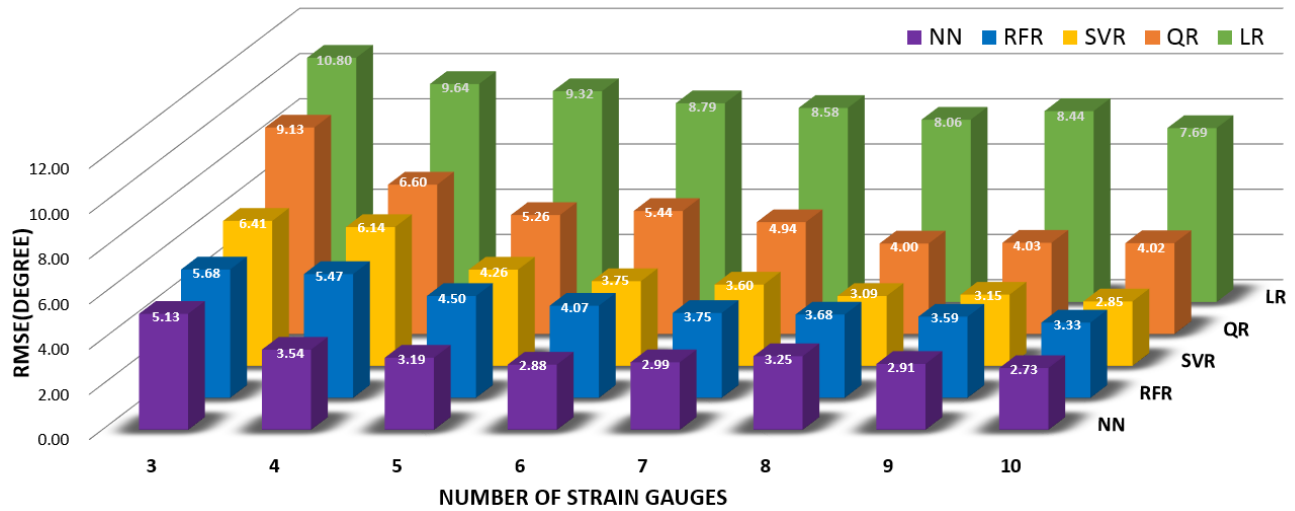


Fig. 8. Comparison between different regression models with varying numbers of target strain gauges.

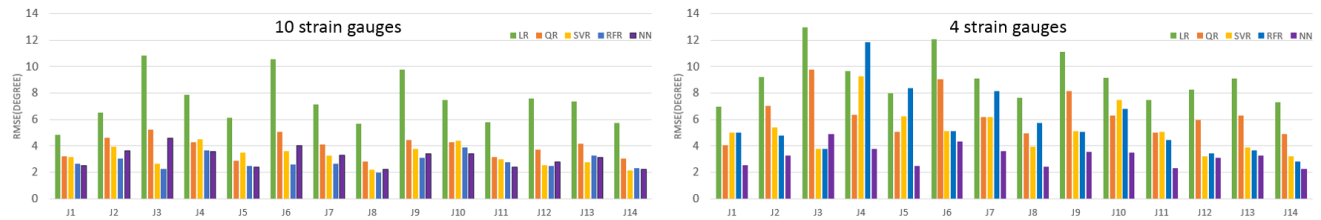


Fig. 9. RMSE of the five regression models using 10 strain gauge data (left) or 4 strain gauge data (right).

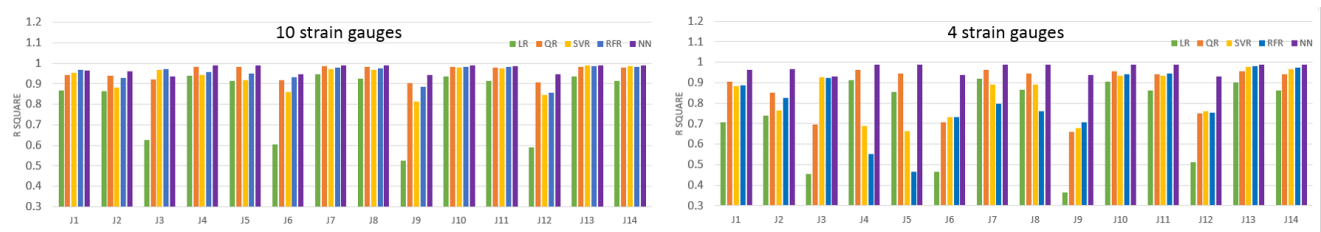


Fig. 10. R^2 of five regression models using 10 strain gauge data (left) or 4 strain gauge data (right).

References

- [1] Kramer, James F., William R. George, and Peter Lindener. "Strain-sensing goniometers, systems and recognition algorithms." U.S. Patent 5,280,265, issued January 18, 1994.
- [2] Lorusso, Federico, Enzo Pasquale Scilingo, Mario Tesconi, Alessandro Tognetti, and Danilo De Rossi. "Strain sensing fabric for hand posture and gesture monitoring." *IEEE Transactions on Information Technology in Biomedicine* 9, no. 3 (2005): 372-381.
- [3] Lei, J. I. N. G., Z. H. O. U. Yinghui, Zixue Cheng, and W. A. N. G. Junbo. "A recognition method for one-stroke finger gestures using a MEMS 3D accelerometer." *IEICE transactions on information and systems* 94, no. 5 (2011): 1062-1072.
- [4] Chen, Feng-Sheng, Chih-Ming Fu, and Chung-Lin Huang. "Hand gesture recognition using a real-time tracking method and hidden Markov models." *Image and vision computing* 21, no. 8 (2003): 745-758.
- [5] Bretzner, Lars, Ivan Laptev, and Tony Lindeberg. "Hand gesture recognition using multi-scale colour features, hierarchical models and particle filtering." In *Automatic Face and Gesture Recognition, 2002. Proceedings. Fifth IEEE International Conference on*, pp. 423-428. IEEE, 2002.
- [6] Ren, Zhou, Jingjing Meng, Junsong Yuan, and Zhengyou Zhang. "Robust hand gesture recognition with kinect sensor." In *Proceedings of the 19th ACM international conference on Multimedia*, pp. 759-760. ACM, 2011.
- [7] Biswas, Kanad K., and Saurav Kumar Basu. "Gesture recognition using microsoft kinect." In *Automation, Robotics and Applications (ICARA), 2011 5th International Conference on*, pp. 100-103. IEEE, 2011.
- [8] Marin, Giulio, Fabio Dominio, and Pietro Zanuttigh. "Hand gesture recognition with leap motion and kinect devices." In *Image Processing (ICIP), 2014 IEEE International Conference on*, pp. 1565-1569. IEEE, 2014.
- [9] ProGlove, "1st smart glove for industries," ProGlove, 2015. [Online]. Available: <http://www.proglove.de>. Accessed: Mar. 2, 2017.
- [10] Cyber Glove Systems, "MoCap Glove System" [Online]. Available: <http://www.cyberglovesystems.com>. Accessed: Mar. 11, 2018.
- [11] M. T. Review, "Gest," 2015. [Online]. Available: <https://gest.co>. Accessed: Mar. 2, 2017.
- [12] K. M, "Myo gesture control Armband," 2013. [Online]. Available: <https://www.myo.com>. Accessed: Mar. 2, 2017.
- [13] "Leap motion," Leap Motion, 2017. [Online]. Available: <https://www.leapmotion.com>. Accessed: Mar. 2, 2017.
- [14] B. V. Guide, "Samsung rink," Buy VR Guide, 2017. [Online]. Available: <http://www.buyvrguide.com/vr-controllers/samsung-rink/>. Accessed: Mar. 2, 2017.
- [15] Weichert F, Bachmann D, Rudak B, Fisseler D. Analysis of the Accuracy and Robustness of the Leap Motion Controller. *Sensors* (Basel, Switzerland). 2013;13(5):6380-6393. doi:10.3390/s130506380.
- [16] Zappi, Piero, Thomas Stiefmeier, Elisabetta Farella, Daniel Roggen, Luca Benini, and Gerhard Troster. "Activity recognition from on-body sensors by classifier fusion: sensor scalability and robustness." In *Intelligent Sensors, Sensor Networks and Information, 2007. ISSNIP 2007. 3rd International Conference on*, pp. 281-286. IEEE, 2007.
- [17] Lee, Seon-Woo, and Kenji Mase. "Activity and location recognition using wearable sensors." *IEEE pervasive computing* 1, no. 3 (2002): 24-32.
- [18] Mattmann, Corinne, Oliver Amft, Holger Harms, Gerhard Troster, and Frank Clemens. "Recognizing upper body postures using textile strain sensors." In *Wearable Computers, 2007 11th IEEE International Symposium*

- on, pp. 29-36. IEEE, 2007.
- [19] Kern, Nicky, Bernt Schiele, and Albrecht Schmidt. "Multi-sensor activity context detection for wearable computing." In European Symposium on Ambient Intelligence, pp. 220-232. Springer Berlin Heidelberg, 2003.
- [20] J. Christoffersen, "Strain gauges: Electrical instrumentation signals - electronics textbook,". [Online]. Available: <https://www.allaboutcircuits.com/textbook/direct-current/chpt-9/strain-gauges/>. Accessed: Feb. 28, 2017.
- [21] Zhou, Quan, Wenlin Chen, Shiji Song, Jacob R. Gardner, Kilian Q. Weinberger, and Yixin Chen. "A reduction of the elastic net to support vector machines with an application to gpu computing." arXiv preprint arXiv:1409.1976 (2014).
- [22] Andrea Tagliasacchi, Matthias Schrder, Anastasia Tkach, Sofien Bouaziz, Mario Botsch, Mark Pauly, "Robust Articulated-ICP for Real-time Hand Tracking", Computer Graphics Forum (Proceedings of SGP), 2015
- [23] Wentai Zhang, Jonelle Z. Yu, Fangcheng Zhu, Yifang Zhu, Nurcan Gecer Ulu, Batuhan Arisoy, Levent Burak Kara. (2018). High Degree of Freedom Hand Pose Tracking Using Limited Strain Sensing and Optical Training. ASME International Design Engineering Technical Conferences/CIE., 2018, Quebec City, Canada.